Induction of Endogenous Interferon Tau Gene Transcription by CDX2 and High Acetylation in Bovine Nontrophoblast Cells 1

Authors: Sakurai, Toshihiro, Sakamoto, Atsushi, Muroi, Yoshikage, Bai, Hanako, Nagaoka, Kentaro, et al.

Source: Biology of Reproduction, 80(6) : 1223-1231

Published By: Society for the Study of Reproduction

URL: https://doi.org/10.1095/biolreprod.108.073916

BIOLOGY OF REPRODUCTION **80,** 1223–1231 (2009)
Published online before print 11 February 2009.
DOI 10.1095/biolreprod.108.073916

Induction of Endogenous Interferon Tau Gene Transcription by CDX2 and High Acetylation in Bovine Nontrophoblast Cells[1]

Toshihiro Sakurai,[3] Atsushi Sakamoto,[3,4] Yoshikage Muroi,[3] Hanako Bai,[3] Kentaro Nagaoka,[3] Kazuhiro Tamura,[4] Toru Takahashi,[5] Kazuyoshi Hashizume,[6] Miki Sakatani,[7] Masashi Takahashi,[7] James D. Godkin,[8] and Kazuhiko Imakawa[2,3]

Laboratory of Animal Breeding,[3] Veterinary Medical Sciences, Graduate School of Agricultural and Life Sciences, The University of Tokyo, Bunkyo-ku, Tokyo, Japan
Laboratory of Molecular Pharmacology,[4] Tokyo University of Pharmacology and Life Sciences, Hachioji, Tokyo, Japan
Reproductive Biology Research Unit,[5] National Institute of Agrobiological Sciences, Tsukuba, Ibaraki, Japan
Department of Veterinary Medicine,[6] Iwate University, Morioka, Iwate, Japan
Research Team for Effects of Climate Change on Agriculture,[7] National Agricultural Research Center for Kyushu Okinawa Region, Kumamoto, Japan
Department of Animal Sciences,[8] University of Tennessee, Knoxville, Tennessee

ABSTRACT

Interferon tau gene (*IFNT*) is expressed only by mononuclear trophectoderm cells in ruminant ungulates. To our knowledge, its epigenetic regulation and interaction with trophectoderm lineage-specific caudal-related homeobox 2 transcription factor (CDX2) have not been characterized. Herein, we studied differences in chromatin structures and transcription of endogenous bovine *IFNT* in bovine trophoblast BT-1 and CT-1 cells and in nontrophoblast MDBK cells. Transcripts from endogenous *IFNT* and *CDX2* genes were found in BT-1 and CT-1 cells but not in MDBK cells. Chromatin immunoprecipitation study revealed that CDX2 binding sites exist in proximal upstream regions of *IFNT* (IFN-tau-c1). Endogenous *IFNT* transcription in BT-1 cells was increased with *CDX2* overexpression but was reduced with short interfering RNA specific for the *CDX2* transcript. In chromatin immunoprecipitation studies, histone H3K18 acetylation of *IFNT* was higher in CT-1 cells than in MDBK cells, while histone H3K9 methylation was lower in CT-1 cells than in nontrophoblast cells. In MDBK cells (but not in CT-1 cells), histone deacetylases were bound to *IFNT*, which was reversed with trichostatin A treatment; treatment with trichostatin A and *CDX2* then increased *IFNT* mRNA levels that resulted from abundant *CDX2* mRNA expression. These data provide evidence that significant increase in endogenous *IFNT* transcription in MDBK cells (which do not normally express IFNT) can be induced through *CDX2* overexpression and high H3K18 acetylation, but lowering of H3K9 methylation could also be required for the degree of *IFNT* transcription seen in trophoblast cells.

[1]Supported by Grants-in-aid for Scientific Research (18108004) from the Japan Society for the Promotion of Science and by the Program for Promotion of Basic Research Activities for Innovative Bioscience (BRAIN).
[2]Correspondence: Kazuhiko Imakawa, Laboratory of Animal Breeding, Veterinary Medical Sciences, Graduate School of Agricultural and Life Sciences, The University of Tokyo, Bunkyo-ku, Tokyo 113-8657, Japan. FAX: 81 3 5841 8180; e-mail: akaz@mail.ecc.u-tokyo.ac.jp

Received: 1 October 2008.
First decision: 23 October 2008.
Accepted: 27 January 2009.

eISSN: 1259-7268 http://www.biolreprod.org
ISSN: 0006-3363

acetylation, bovine, chromatin, conceptus, embryo, gene regulation, IFNT, implantation, methylation, trophoblast cells

INTRODUCTION

Interferon tau (IFNT), secreted by mononuclear trophectoderm cells of peri-implantation conceptuses into the uterine lumen, is the major cytokine implicated in the process of maternal recognition of pregnancy in ruminant ungulates [1, 2]. IFNT decreases endometrial oxytocin and estrogen receptors, which attenuates episodic prostaglandin F2α secretion, resulting in prevention of luteolysis [3, 4]. IFNT secretion exhibits temporal and spatial limits in that its production is restricted to trophectoderm cells during the peri-implantation period [5, 6]. In ewes, IFNT production begins on Day 8 of pregnancy (estrus is Day 0), and the quantity of its production seems to parallel the degree of trophoblast elongation [7, 8]. Its secretion peaks on Day 16, just before attachment of the conceptus to the uterine epithelium, and declines subsequently [8, 9]. By Day 22, when placenta formation is initiated, IFNT is no longer detected [5]. Bovine and caprine conceptuses exhibit a similar cell-specific and temporal pattern of IFNT expression [10–12].

Although *IFNT* mRNA and genes were discovered more than two decades ago, the molecular mechanisms by which IFNT expression is regulated in a temporal and spatial manner are not well understood. By analyzing the 5′ upstream regions of *IFNT*, transcription factors such as activating protein 1 (AP1, official symbol JUN) and DNA-binding ETS domain ETS2 were found to be responsible for increased *IFNT* transcription [13–16]. In addition to trophoblasts and placenta, however, transcription factors such as JUN and ETS2 are expressed in a wide variety of tissues and cell types [17, 18]. Moreover, the transcription coactivator cAMP-response element binding protein (CREB)-binding protein (CREBBP), which has histone acetyltransferase (HAT) function, was shown to regulate ovine *IFNT* expression [19, 20]. It is still unclear why IFNT is expressed only in trophoblast and how its production is initiated and terminated within a short period of development. Therefore, it is thought that the unique *IFNT* expression could be controlled not only by transcription factors but also by chromatin modification.

Epigenetic alterations such as variation in DNA methylation and covalent histone modification regulate gene expression by altering chromatin conformation. DNA methylation usually occurs at cytosine residues within CG dinucleotides or CNG

TABLE 1. Oligonucleotide primer sequences for ChIP assay and nucleotide sequences for *CDX2* siRNA.

Parameter (GenBank accession no.)	Location	Sequence[a]
ChIP assay		
Bovine *IFNT* (AF238613)		
Region 1	+314 to +520 bp	F: 5′-GCTCCAGCAGTGCTTCAACC-3′
		R: 5′-ACATGGATGCCCTGGAAGTA-3′
Region 2	−240 to −47 bp	F: 5′-CATAACTTCAGCCTTTATTT-3′
		R: 5′-ATTCATTATCCAAAAATTTC-3′
Region 3	−755 to −560 bp	F: 5′-GAAATCCAGGGGTTGGTGAT-3′
		R: 5′-GTGGAGTATTTCCCGCCATA-3′
siRNA		
CDX2 (XM_871005)		
siRNA #1	609 to 627 bp in ORF	5′-GGAGUUUCACUACAGUCGCTT-3′
siRNA #2	679 to 697 bp in ORF	5′-GAGAGGCAGGUUAAAAUUUTT-3′
siRNA #3	744 to 762 bp in ORF	5′-GUUGCAACAGCAGCAGCAATT-3′
EGFP (EU056363)		
siRNA (control)		5′-GACGACGGCAACUACAAGACC-3′

[a] F, forward; R, reverse.

trinucleotides and generally opposes transcription [21, 22]. Changes in the degree of DNA methylation in the upstream sequences of ovine *IFNT* could be one of the major mechanisms leading to downregulation of its expression and possibly its silencing in nonconceptus tissues [23]. In addition to DNA methylation, histone posttranslational modifications such as acetylation and methylation are correlated with positive or negative transcriptional status of various genes [24]. Acetylation of lysine residues is controlled by specific HATs and histone deacetylases (HDACs). Four lysine residues (K9, K14, K18, and K56) of histone H3 (H3K9, H3K14, H3K18, and H3K56, respectively) and four lysine residues (K5, K8, K13, and K16) of histone H4 (H4K5, H4K8, H4K13, and H4K16, respectively) are acetylated by specific HATs [25]. It has been demonstrated that histone acetylation/deacetylation alters chromosome structure, which in turn affects accession of transcription factors to DNA sequences. Histone posttranslational modifications are also modified through histone methylation. Five lysine residues (K4, K9, K27, K36, and K79) of histone H3 (H3K4, H3K9, H3K27, H3K36, and H3K79, respectively) and K20 of histone H4 (H4K20) are methylated by the relevant histone methyltransferases, are demethylated by histone demethylases, and are associated with repression and activation of transcription [25]. It is generally believed that methylated H3K4, H3K36, and H3K79 are associated with active transcription, while methylated H3K9, H3K27, and H4K20 are associated with a transcriptionally inactive state [24]. Moreover, it was demonstrated that H3K9 methylation is mechanistically linked to DNA methylation [26]. H3K9 methylation is considered crucial for heterochromatin assembly, resulting in specific binding of heterochromatin protein 1 (HP1, official symbol CBX5) to methylated H3K9 [27, 28], whereas H3K4 methylation occurs preferentially within transcriptionally competent chromatin [29]. However, modification of the chromatin structure of *IFNT*, 5′ upstream regions, and open reading frame (ORF) that are associated with the degree of *IFNT* transcription has not been studied in much detail.

It was shown that caudal-related homeobox 2 transcription factor (CDX2) is expressed in ovine and bovine trophoblasts during the conceptus elongation period [30, 31]. In fact, overexpression of *CDX2* along with *JUN* and *ETS2* in human choriocarcinoma JEG3 cells was effective in increasing the degree of transcription of an ovine *IFNT* reporter construct [31]. These results suggest that CDX2 could be a key element that determines trophoblast cell-specific activation of *IFNT* expression. In this study, we examined the importance of CDX2 and chromatin structures in endogenous *IFNT* transcription in bovine trophoblast-derived BT-1 [32] and CT-1 [33] cells and in nontrophoblast bovine kidney MDBK cells. Our findings should lead to a better understanding of how trophectoderm expression of a conceptus gene is regulated during the establishment of pregnancy.

MATERIALS AND METHODS

Cell Cultures and Their Treatment

Bovine trophoblast BT-1 [32] and CT-1 [33] cells (kindly provided by Dr. A. Ealy, University of Florida, Gainesville, FL) were established from in vitro matured and fertilized blastocysts and were cultured without feeder cells. BT-1 cells were cultured on plastic plates coated with type I collagen (Nitta Gelatin, Osaka, Japan) in Dulbecco modified Eagle (DME)/F12 medium (Invitrogen, Carlsbad, CA) supplemented with 10% v/v fetal bovine serum (FBS; JRH Biosciences, Lenexa, KS) and antibiotics/antimycotic solution (Invitrogen) at 37°C in air with 5% CO_2. Cells were mechanically dissociated with a pipette, and the clumps were plated on plastic plates in culture medium as already described. CT-1 cells were maintained at 37°C in air with 5% CO_2 in DME medium containing 10% v/v FBS supplemented with 4.5 g/L of D-glucose, nonessential amino acids, 2 mM glutamine, 2 mM sodium pyruvate, 55 μM β-mercaptoethanol, and antibiotic/antimycotic solution (all from Invitrogen). CT-1 cells were scraped from the plates and passed through a small-bore needle to generate small clumps of cells before reseeding. MDBK cells, a bovine kidney-derived epithelial cell line (American Type Culture Collection, Rockville, MD), were grown in DME medium supplemented with 10% v/v FBS and antibiotics at 37°C in 5% CO_2 in air. Bovine ovarian cumulus granulosa (oCG) cells were obtained from ovarian follicles that had been collected at a local abattoir, and ear-derived fibroblast (EF) cells were obtained from biopsied ear skin of 4-mo-old Japanese black bulls. Both cells were cultured in DME medium containing 5% v/v FBS (JRH Biosciences) and antibiotics (Invitrogen) at 37°C in air with 5% CO_2. Each cell type was serum starved for 24 h before treatment. In addition to bovine cells, human choriocarcinoma JEG3 cells (American Type Culture Collection) were cultured in DME medium supplemented with 10% FBS (JRH Biosciences) and antibiotics (Invitrogen) as described previously [31].

PCR Analysis and Real-Time PCR Analysis

Total RNA was isolated from cultured cells of each type using Isogen (Nippon Gene, Tokyo, Japan) according to the protocol provided by the manufacturer. Isolated RNA (250 ng) was converted to cDNA using SuperScript II (Invitrogen) and oligo(dT) primers in a 20-μl reaction volume, and the resulting cDNA (RT template) was stored at 4°C until use. The cDNA reaction mixture was diluted 1:10 using DNase and RNase-free molecular biology grade water, and 3 μl was taken for each amplification reaction. The PCR was performed using 0.5 U of ExTaq polymerase (Takara Biomedicals, Tokyo, Japan), 1× ExTaq buffer, 0.2 μM of the oligonucleotide primers listed in Table 1, and 0.2 mM deoxyribonucleotide triphosphate in a final volume of 20 μl. The thermal profile for PCR was at 95°C for 10 min, followed by 28 cycles of 95°C for 10 sec, 60°C for 30 sec, and 72°C for 30 sec. The PCR

TABLE 2. Oligonucleotide primer sequences used for RT-PCR analysis.

Name	GenBank accession no.	Primer sequence[a]	Length (bp)
Bovine *IFNT*	AF238613	F: 5′-CATCTTCCCCATGGCCTTCG-3′ R: 5′-TCATCTCAAAGTGAGTTCAG-3′	206
CDX2	XM_871005	F: 5′-GCCACCATGTACGTGAGCTAC-3′ R: 5′-ACATGGTATCCGCCGTAGTC-3′	140
ETS2	NM_001080214	F: 5′-GTGGGCCTATCCAGCTGTGG-3′ R: 5′-TTCCCTGACGTCTTGTGGAT-3′	227
JUN	NM_010591	F: 5′-GAGTCTCAGGAGCGGATCAA-3′ R: 5′-TGAGTTGGCACCCACTGTTA-3′	225
CREBBP	XM_581740	F: 5′-CAAGGAGCTGCCCTACTTTG-3′ R: 5′-TTTTTCTGGGCGTTCTTGCT-3′	226
ACTB	BC102948	F: 5′-CTCTTCCAGCCTTCCTTCCT-3′ R: 5′-GGGCAGTGATCTCTTTCTGC-3′	177

[a] F, forward; R, reverse.

products were separated on a 1.5% agarose gel containing ethidium bromide and were visualized under UV light.

Reverse-transcribed cDNA (3 μl) was subjected to real-time PCR amplification using 0.5 U of ExTaq HS polymerase (Takara Biomedicals), 1× ExTaq HS buffer, 0.2 μM of the oligonucleotide primers listed in Table 1, 0.2 mM deoxyribonucleotide triphosphate, SYBR green (SYBR Green I Nucleic Acid Gel stain; Takara Biomedicals) as a fluorescence intercalater, and Rox reference dye (Invitrogen) in a final volume of 20 μl. The PCR amplification was performed on an 7900HT real-time PCR system (Applied Biosystems, Foster City, CA). The thermal profile for real-time PCR was 95°C for 10 min, followed by 40 cycles of 95°C for 10 sec, 60°C for 20 sec, and 72°C for 40 sec. Average cycle threshold (Ct) values for *IFNT*, *CDX2*, *ETS2*, *JUN*, and *CREBBP* were calculated and normalized to Ct values for *ACTB* [34]. Each run was completed with a melting curve analysis to confirm the specificity of amplification and the absence of primer dimers.

Plasmid Construction, Short Interfering RNAs, and Transfection

A mouse *Cdx2* expression plasmid in pRC-cytomegalovirus was kindly provided by Dr. EunRan Suh, University of Pennsylvania School of Medicine, Philadelphia, PA. *Cdx2* cDNA was subcloned into the pSG5 plasmid (Invitrogen), resulting in construction of the pSG5-*Cdx2* plasmid. Constructs containing each of 14 CDX2 sites of mutated bovine IFNT were prepared by an inverse PCR procedure as previously described [31] with appropriate primers that included mutation; the CDX2 recognition site was mutated from 5′-TTTACTG-3′ to 5′-TTTTGTG-3′. Nucleotide structures of these constructs were confirmed by DNA sequencing. Transient transfection and luciferase activity measurements were performed in JEG3 cells as previously described [31]. *CDX2* short interfering RNAs (siRNAs) (whose nucleotide structures were designed using the siDirect program; RNAi Co., Ltd., Tokyo, Japan), were prepared commercially (Sigma-Aldrich, St. Louis, MO). The nucleotide sequence of bovine *CDX2* (XM_871005) was used to design three different siRNAs for *CDX2* coding regions, while an unrelated sequence of *EGFP* (EU056363) was used as a negative control (Table 1).

To evaluate the effects of mouse *Cdx2* overexpression or its knockdown on the abundance of bovine *IFNT* mRNA, the pSG5-*Cdx2* or *CDX2* siRNA was transfected into BT-1 cells using Lipofectamine 2000 reagents (Invitrogen) according to the procedure recommended by the manufacturer. The procedure for the transfection was essentially as previously described [31]. Concentrations of each siRNA had been determined before the experiment. The pSG5-*Cdx2* siRNA (2 μg [seeded on a six-well dish]) and *CDX2* siRNA (50 nM [seeded on a 24-well dish) were transfected into BT-1 cells for 48 h, from which tRNA was extracted and reverse transcribed to cDNA. The yielded cDNAs were subjected to real-time PCR analysis with the primers listed in Table 2 for determination of bovine *IFNT* and *CDX2* mRNA levels. Average Ct values for bovine *IFNT* and *CDX2* were calculated and normalized to Ct values for *ACTB*.

Chromatin Immunoprecipitation Assay

Chromatin immunoprecipitation (ChIP) assays were performed using the ChIP assay kit (Upstate Biotechnology, Lake Placid, NY) following the protocol provided by the manufacturer. Briefly, bovine cells (~5×10^6 cells/10-cm dish) were treated with or without 200 nM trichostatin A (TSA; Wako, Tokyo, Japan). Twenty-four hours after initiation of TSA treatment, the cells were transfected with pSG5 only or with pSG5-*Cdx2* (4 μg) and cultured for 48 h, resulting in 72 h of total TSA treatment. Potential protein-DNA complexes in these cells were cross-linked with 1% formaldehyde for 20 min, washed with chilled PBS, resuspended in 200 μl of SDS lysis buffer, and sonicated six times for 10 sec each at 60% maximum setting of the sonicator (Handy Sonic UR-20P; Tomy Seiko Co., Ltd., Tokyo, Japan). The supernatant of sonicated cells was diluted 10-fold to a total volume of 2 ml, and 1% (20 μl) of diluted lysates was used for total genomic DNA as input DNA control. To reduce nonspecific ChIP signals, the remaining cell lysates were subjected to an immunoclearing procedure to which 75 μl of protein A agarose/salmon sperm DNA (50% slurry) (Upstate Biotechnology) was added, and sample tubes were agitated at 4°C for 30 min. Immunoprecipitation was then performed overnight at 4°C with rabbit polyclonal antihistone H3 acetyl K18 (H3K18ac) antibody (2 μg; ab1191), rabbit polyclonal antihistone H3 monomethyl K9 (H3K9me) antibody (5 μg; ab9045), rabbit polyclonal antihistone H3 dimethyl K9 (H3K9me2) antibody (5 μg; ab1220), rabbit polyclonal antihistone H3 trimethyl K4 (H3K4me3) antibody (4 μg; ab1012), mouse monoclonal antiHDAC1 antibody (2.5 μg; ab31263), or mouse monoclonal antiHDAC2 antibody (2.5 μg; ab51832 [all from Ab Chem, Inc., Ville St-Laurent, QC, Canada]) or with mouse monoclonal antihuman CDX2 antibody (4 μg; BioGenex, San Ramon, CA). Normal rabbit IgG (Santa Cruz Biotechnology, Santa Cruz, CA) or normal mouse IgG (Cell Signaling Technology, Inc., Danvers, MA) instead of antibody was used as a negative control. Using the ChIP assay protocol provided by the manufacturer, concentrations of each antibody were examined and validated for these assays. Precipitates were washed sequentially for 5 min each in low-salt, high-salt, and lithium chloride immune complex wash buffers and were finally washed twice with Tris/edetic acid buffer. Histone complexes were then eluted from the antibody by freshly prepared elution buffer (1% SDS, 0.1 M $NaHCO_3$, and 10 mM dithiothreitol). Protein-DNA cross-links (including the input DNA control samples) were reversed by 5 M NaCl at 65°C for 4 h, followed by proteinase K (Invitrogen) digestion at 45°C for 2 h. The DNA fragments were extracted with phenol and chloroform, precipitated with ethanol and 0.3 M sodium acetate (pH 8.2), and resuspended in 30 μl of Tris/edetic acid buffer, from which 3 μl was used for PCR (35 cycles) with the primers listed in Table 2. The PCR products were separated on a 1.5% agarose gel containing ethidium bromide and were visualized under UV light. The band intensity was determined using NIH Image analyzer (National Institutes of Health, Bethesda, MD), and each value was normalized against the relevant input bands.

Statistical Analysis

All quantitative data were subjected to least squares ANOVA using SAS software (SAS Institute, Cary, NC). The model used in the least squares ANOVA included treatment and replicate as sources of variation. The SEMs in the figures were derived from this analysis. When a significant effect of treatment was detected ($P < 0.05$), the data were analyzed using Dunnett test for multiple comparisons. In these analyses, treatment was considered an independent source of variation, and replicate was considered a dependent source.

RESULTS

Abundance of Bovine IFNT, CDX2, and Other Transcription Factor mRNAs in Various Bovine Cell Lines

Bovine *IFNT*, *CDX2*, *ETS*2, *JUN*, and *CREBBP* mRNA expressions in BT-1, CT-1, MDBK, EF, and oCG bovine cell lines are shown in Figure 1. The results indicated that

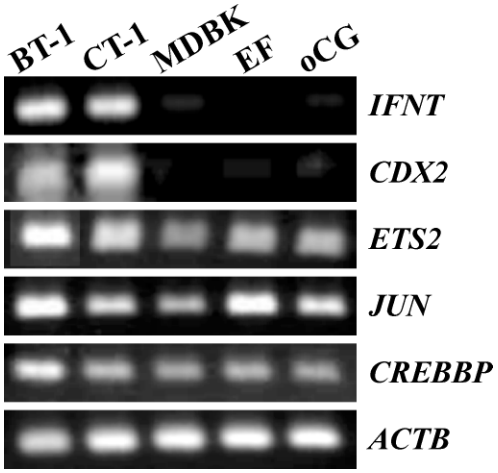

FIG. 1. Abundance of *IFNT, CDX2, JUN, ETS2,* and *CREBBP* mRNA in bovine cell lines. Total RNAs isolated from trophoblast BT-1 or CT-1 cells and from nontrophoblast MDBK, EF, or oCG cells were reverse transcribed to cDNA and then subjected to PCR analysis using the primers listed in Table 1.

expression of *IFNT* and *CDX2* mRNA was found in trophoblast BT-1 and CT-1 cells but not in nontrophoblast MDBK, EF, or oCG cells.

Binding of CDX2 to the Upstream Region of Bovine IFNT

ChIP assay was performed to determine the CDX2 binding site on bovine *IFNT* (IFN-tau-c1) in BT-1 cells (Fig. 2A). In the upstream region of bovine *IFNT*, CDX2 binding sites in region 2 (−240 to −47 bp) and region 3 (−755 to −560 bp) were identified in BT-1 cells, whereas no CDX2 binding site was found in the ORF region (314–520 bp). In addition, *CDX2* overexpression seemed to increase the ChIP signal, particularly the CDX2 binding site in region 3. These results indicated that the CDX2 binding sites on bovine *IFNT* seemed to be functional in trophoblast BT-1 cells.

Region 2 of bovine *IFNT* represents CDX2-rich regions, having at least 14 potential CDX2 binding sites (Supplemental Fig. S1 available at www.biolreprod.org). One point mutation was introduced to each of these sites. In transient transfection experiments in CT-1 cells, all constructs with mutated CDX2 sites had reduced luciferase activity (one half to one fourth of wild-type constructs [results not shown]). Together with CDX2 binding by ChIP assay, these data indicated that each of 14 CDX2 sites was functional.

Endogenous Bovine IFNT *mRNA Levels Following Changes in* CDX2 *Expression in BT-1 Cells*

It was previously shown that a −654-bp ovine *IFNT* construct was transactivated more than 30-fold in JEG3 cells by cotransfection of *Jun*, *Ets2*, and *Cdx2* [31]. In lieu of heterologous transfection studies [13–16, 18], levels of endogenous bovine *IFNT* transcription were studied in BT-1 cells that had been transfected with the pSG5-*Cdx2* expression construct. The results revealed that overexpression of *Cdx2* in BT-1 cells increased bovine *IFNT* mRNA levels more than 5-fold ($P < 0.01$) compared with control cells, into which the pSG5 plasmid without *Cdx2* (mock) had been transfected (Fig. 2B [left]).

To determine whether downregulation of *CDX2* reduces endogenous bovine *IFNT* transcription, three different siRNAs for bovine *CDX2* mRNA were designed and synthesized (Table 1). BT-1 cells were then transiently transfected with one of these *CDX2* siRNAs or with an *EGFP* siRNA as a negative control. Although two of these siRNAs (siRNA 1 and siRNA 2) reduced *CDX2* mRNA ($P < 0.05$ and $P < 0.01$, respectively), *CDX2* siRNA 2 more effectively reduced the amount of *CDX2* mRNA than *CDX2* siRNA 1, which in turn resulted in the reduction of endogenous bovine *IFNT* mRNA (Fig. 2B [right]). The effect of the *CDX2* siRNAs was limited to *CDX2* mRNA and bovine *IFNT* mRNA expression, as *ETS2*, *JUN*, *CREBBP*, and *POU5F1* mRNA levels were unaffected by this treatment (data not shown). Figure 2B illustrates that the transcription of bovine *IFNT* was regulated by the degree of *CDX2* transcription.

Histone Methylation and Acetylation of Bovine IFNT *in CT-1 and MDBK Cells*

During experiments, we noticed that BT-1 cells with more than 300 passages were losing or had lost endogenous IFNT transcription and/or production. Instead of BT-1 cells, CT-1 cells were therefore used for the remaining experiments, as CT-1 cells at that point gave similar (if not the same) results compared with those initially found in BT-1 cells.

To elucidate whether the status of histone H3 methylation and acetylation determines the degree of bovine *IFNT* transcription, the ChIP assay was executed in bovine trophoblast and nontrophoblast cells using various histone antibodies. DNA-protein complexes were treated with antibodies against H3K18ac, H3K9me, H3K9me2, H3K4me3, or rabbit IgG (as a negative control) (Fig. 3). The degree of H3K18 acetylation in region 2 of bovine *IFNT* was higher in trophoblast CT-1 cells than in nontrophoblast MDBK cells (control). The degree of H3K9 dimethylation in region 1 (314–520 bp) and region 2 (−240 to −47 bp) was higher in MDBK cells (control) than in CT-1 cells. In addition, H3K4 methylation seemed to be associated with bovine *IFNT* expression in CT-1 cells but not in MDBK cells (control). The status of histone H3 methylation and acetylation in oCG and EF cells was the same as that in MDBK, and the status of these in BT-1 cells was also the same as that in CT-1 cells (data not shown). To determine the effect of TSA treatment on bovine *IFNT* transcription, changes in the status of histone acetylation and methylation on bovine *IFNT* in MDBK cells were studied following treatment with 200 nM TSA. In TSA treatment, the degree of H3K18 acetylation in region 1 and region 2 of bovine *IFNT* and of H3K4 trimethylation in region 1 seemed to increase in MDBK cells (TSA treatment), while H3K9 dimethylation was unchanged. These data suggest that H3K18 acetylation and H3K4 methylation of bovine *IFNT* are important in its expression, while H3K9 dimethylation in the upstream region where the CDX2 binding site is located, as well as in the ORF region, may be associated with suppression of bovine *IFNT* transcription in nontrophoblast cells.

HDAC1 and HDAC2 Binding to Bovine IFNT *in CT-1 and MDBK Cells*

Because methylated H3K9 recruits repressing effector proteins, including HDAC complexes [24, 27, 28], the presence and/or binding of HDACs on bovine *IFNT* was studied using antibodies against HDAC1 and HDAC2 (Fig. 4). In CT-1 cells, a minute ChIP signal of HDAC1 was detected on the ORF (region 1), while HDAC2 was not expressed in either region. In MDBK cells, ChIP signals of HDAC1 and HDAC2 were detected in both regions. In addition, TSA treatment effectively removed HDAC1/HDAC2 from both regions in

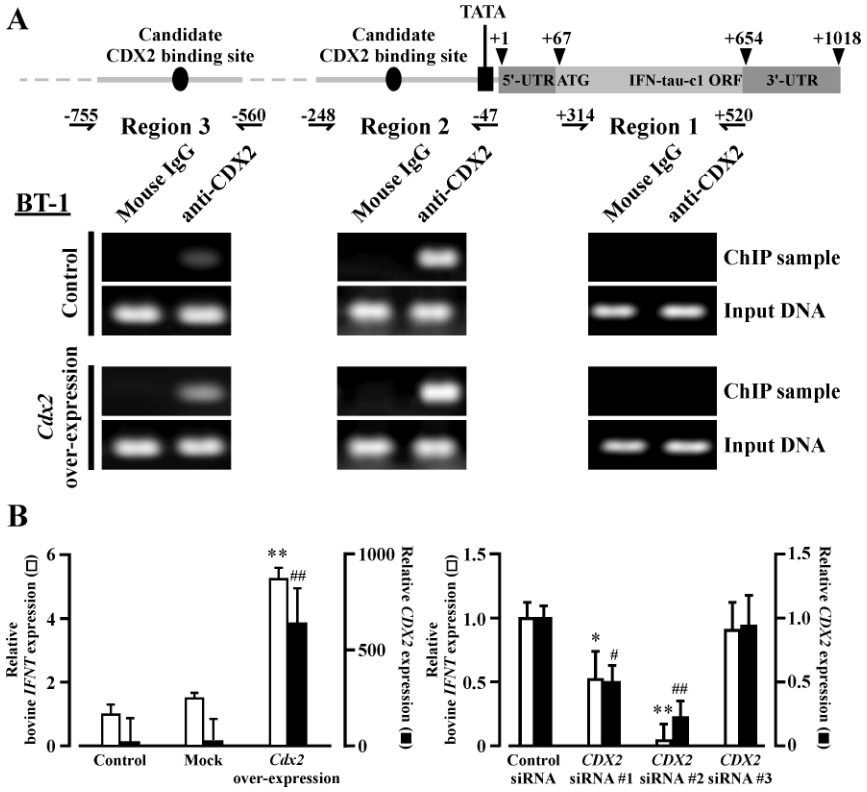

FIG. 2. Binding of transcription factor CDX2 to the upstream region of bovine *IFNT* in BT-1 cells and abundance of endogenous bovine *IFNT* transcripts through changes in *Cdx2* expression. **A**) CDX2 binding in the upstream region of bovine *IFNT* (IFN-tau-c1) is shown by ChIP assay. The protein-DNA complexes that had been formed by formaldehyde treatment were incubated with mouse monoclonal antibody against CDX2, from which the CDX2 binding region was determined by ChIP analysis. The PCR was performed for 35 cycles to amplify the ORF and upstream regions comprising region 1 (314–520 bp), region 2 (−240 to −47 bp), and region 3 (−755 to −560 bp) of bovine *IFNT*. Upper: control (pSG5-only transfection in BT-1 cells); lower: *Cdx2* overexpression (pSG5-*Cdx2* [4 μg] transfection in BT-1 cells [seeded on a 10-cm culture dish]). Results from one of three independent experiments are shown. **B**) Shown on the left is the expression of bovine *IFNT* and *CDX2* mRNA in BT-1 cells following transfection of a *Cdx2* expression construct. BT-1 cells (seeded on a six-well dish) were transfected with pSG5-*Cdx2* (CDX2) (2 μg) and with pSG5 (mock) construct for 48 h, from which tRNA was extracted, reverse transcribed to cDNA, and subjected to real-time PCR analysis for determination of bovine *IFNT* and *CDX2* mRNA levels from endogenous bovine *IFNT* (open bar) and transfected *Cdx2* (solid black bar), respectively. Amounts of bovine *IFNT* and *CDX2* mRNA relative to those from the respective control are shown. There are two y-axes in each graph, with amounts of bovine *IFNT* mRNA on the left y-axis and amounts of *CDX2* mRNA on the right y-axis. Data are presented as means ± SEMs from three independent experiments. $^{**}P < 0.01$ vs. control (IFNT, open bar), $^{\#\#}P < 0.01$ or control (CDX2, solid black bar). Shown on the right is the abundance of bovine *IFNT* mRNA following *Cdx2* siRNA transfection. RNA was extracted from BT-1 cells that had been transfected with CDX2 siRNA 1, siRNA 2, or siRNA 3 (50 nM) or with *EGFP* siRNA (control si). Abundance of bovine *IFNT* and *CDX2* mRNA was detected by real-time PCR. Levels of bovine *IFNT* and *CDX2* mRNA from endogenous bovine *IFNT* (open bar) and transfected *Cdx2* (solid black bar) relative to those from the respective control are shown. Data are presented as means ± SEMs from three independent experiments. $^{*}P < 0.05$, $^{**}P < 0.01$ vs. control si (IFNT, open bar), $^{\#}P < 0.05$, and $^{\#\#}P < 0.01$ vs. control si (CDX2, solid black bar). UTR, untranslated region.

MDBK cells. It seems that the removal of HDAC1/HDAC2 by treatment with TSA to MDBK cells results in increased acetylation of H3K18, as shown in Figure 3. Therefore, in nontrophoblast cell lines in which *IFNT* is not transcribed, the upstream and ORF regions seem have recruited HDACs as negative modifiers.

Effects of CDX2 and TSA Treatment on CDX2 Binding to Bovine IFNT *and the Degree of Its Transcription*

Because the difference in bovine *IFNT* transcription between trophoblast cells and nontrophoblast cells results from a lack of *CDX2* expression (Fig. 1) and its binding to region 2 (Fig. 2A), we assessed binding of CDX2 to the upstream region of bovine *IFNT* in MDBK cells when treated with the pSG5-*Cdx2* construct (4 μg) and with 200 nM TSA (Fig. 5A). Binding of CDX2 to upstream region 2 in bovine *IFNT* was found following pSG5-*Cdx2* transfection and TSA treatment.

Because no CDX2 expression was found in nontrophoblast cell lines (Fig. 1) and because TSA treatment seemed to increase the degree of H3K18 acetylation (Fig. 3), endogenous bovine *IFNT* mRNA levels were determined following TSA treatment or TSA treatment plus *Cdx2* overexpression in MDBK cells (Fig. 5B). Although some increases in endogenous bovine *IFNT* transcripts in MDBK cells were found throughout *Cdx2* overexpression and TSA treatment, the greatest increase in endogenous bovine *IFNT* transcripts and *Cdx2* mRNA from the expression construct was found when MDBK cells were treated with *Cdx2* plus 200 nM TSA. The increase was minimal in *Cdx2* mRNA in MDBK cells that had been treated only with TSA. These results indicate that bovine *IFNT* transcription in nontrophoblast cell lines, in which IFNT expression is normally kept silent, could be induced by TSA treatment, but sufficient induction requires both *Cdx2* overexpression and TSA treatment.

DISCUSSION

IFNT is thought to be hypomethylated during the zygotic stage, suggesting that its transcription could be initiated at any time. However, *IFNT* expression can first be detected at the blastocyst stage. Ezashi et al. [16] reported that *ETS2*-induced

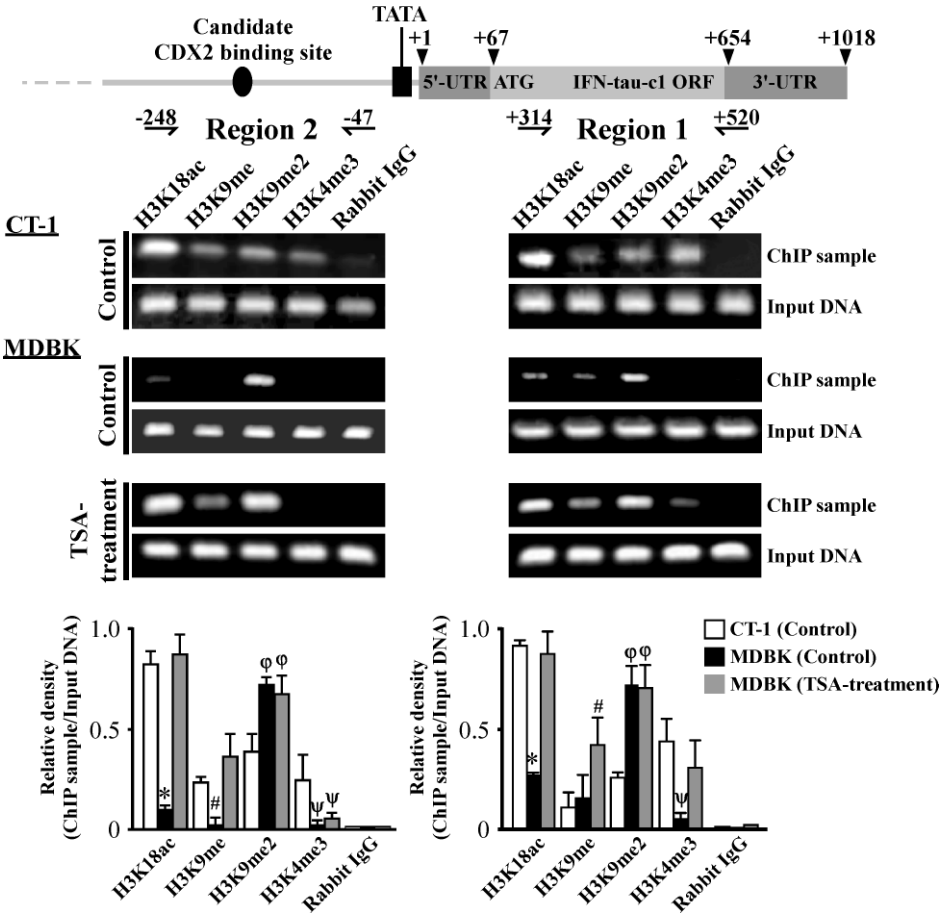

FIG. 3. The degree of histone acetylation and methylation in the upstream and ORF regions of bovine *IFNT* in CT-1 and MDBK cells. Protein-DNA complexes were treated with antibodies against H3K18ac, H3K9me, H3K9me2, H3K4me3, or rabbit IgG, and upstream and ORF regions of nucleotides were amplified using specific primers listed in Table 2. The degree of H3K18 acetylation in region 1 (314–520 bp) and region 2 (−240 to −47 bp) is high in CT-1 cells (upper) and TSA (200 nM)-treated MDBK cells (lower) but not in untreated MDBK cells (middle). The degree of H3K9 dimethylation in region 1 and region 2 is high in TSA-treated and untreated MDBK cells but not in CT-1 cells. ChIP signal densities relative to those of input DNA are quantified and shown in the bar graph. Open bar, CT-1 cells; solid black bar, MDBK cells; solid gray bar, TSA-treated MDBK cells. Results from one of three independent experiments are shown. Data are mean ± SEM from three independent experiments. $^{*}P < 0.01$, $^{\#}P < 0.01$, $^{\varphi}P < 0.01$, and $^{\Psi}P < 0.01$ vs. CT-1 cells (within each antibody). UTR, untranslated region.

transactivation of bovine *IFNT* (*IFNT1*) promoter is repressed by *POU5F1* through direct interaction of ETS2 with POU5F1. Disappearance of POU5F1 in trophectoderm by Day 10 of pregnancy allows ETS2 to assume a positive regulatory role in bovine *IFNT* transcription. However, Imakawa et al. [31] reported that, although ETS2 and JUN activated ovine *IFNT* transcription, overexpression of *Cdx2* plus *Ets2* and *Jun* was most effective in transactivation of an ovine *IFNT* construct. It was shown in the present study that active CDX2 binding sites are present in the proximal upstream region of bovine *IFNT*. It seems that CDX2 expression parallels that of *IFNT* during the peri-implantation period in bovine and ovine trophoblast cells

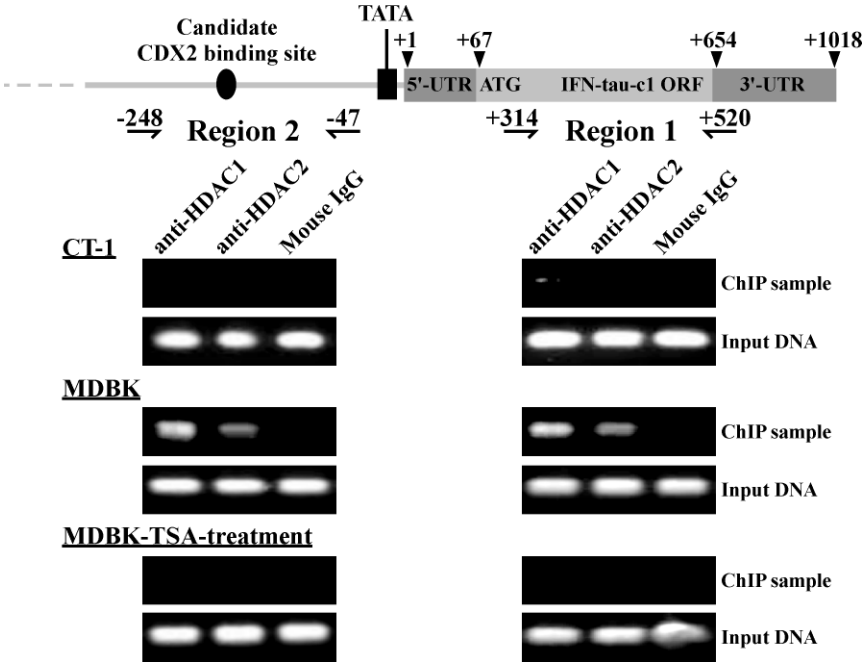

FIG. 4. Examination of HDACs binding in the ORF (region 1) and promoter region (region 2) of bovine *IFNT* in CT-1 and MDBK cells. Whether HDACs were bound to bovine *IFNT* in CT-1 and MDBK cells was examined using ChIP assay with antibodies to HDAC1 and HDAC2. Whereas both HDACs were bound in region 1 and region 2 of bovine *IFNT* in MDBK cells, HDACs were not bound in the promoter region (region 2) of bovine *IFNT* in CT-1 cells or in either region in MDBK cells that had been treated with TSA. Results from one of three independent experiments are shown. UTR, untranslated region.

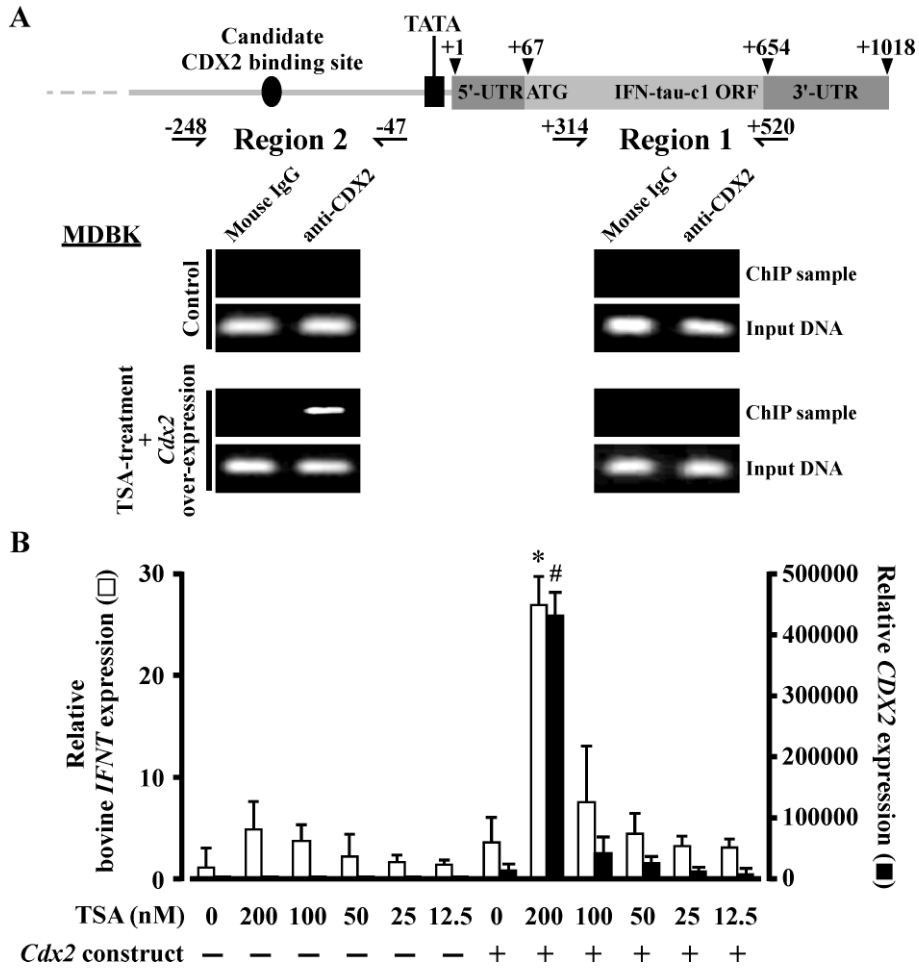

FIG. 5. Binding of CDX2 in the upstream region of bovine *IFNT* and the degree of its transcription in MDBK cells following *Cdx2* and TSA treatment. **A**) The pSG-*Cdx2* construct/TSA treatment was applied to MDBK cells, from which a ChIP assay was performed using the antibody against CDX2. CDX2 binding to region 2 in the upstream region of bovine *IFNT* was detectable following treatment with pSG-*Cdx2* construct plus 200 nM. **B**) Increase in bovine *IFNT* in MDBK cells following TSA treatment or pSG-*Cdx2* construct transfection plus TSA treatment. RNA extracted from MDBK cells that had been treated with pSG-*Cdx2* construct/TSA treatment was reverse transcribed to cDNA and then subjected to real-time PCR for the determination of levels of bovine *IFNT* (open bar) and *CDX2* (solid black bar) mRNA from endogenous bovine *IFNT* and transfected *Cdx2*. An increase in endogenous bovine *IFNT* mRNA was found when MDBK cells were treated with TSA and transfected with the pSG-*Cdx2* construct. The increase in *CDX2* mRNA in MDBK cells that had been treated with TSA only was minimal. Data are presented as means ± SEMs for three independent experiments. $^{*}P < 0.01$ vs. TSA (0 nM)/CDX2 construct (−) (IFNT, open bar), $^{\#}P < 0.01$ vs. TSA (0 nM)/CDX2 construct (+) (CDX2, solid black bar). UTR, untranslated region.

(Sakurai and K. Imakawa, unpublished results). However, it is well known that *CDX2* is not unique to trophectoderm cells, as it is expressed in a number of cell types such as intestinal epithelial cells. CDX2 is activated by phosphorylation via the mitogen-activated protein kinase pathway, resulting in modulation of its transactivating activity [35]. The phosphorylated form of CDX2 is localized in proliferating cells of the crypt in the gut, while the nonphosphorylated form is present in more differentiated cells. The presence of phosphorylated CDX2 has been detected in the blastcyst [36]. Although genes regulated by CDX2 in the blastcyst have not been well characterized, it is probable that phosphorylated CDX2 may regulate *IFNT* expression during the period of conceptus elongation.

In bovine *IFNT* analyzed in this study, there are CpG sites between −900 and −527 bp but no such sites between −526 and −7 bp in its upstream region, whereas CpG sites are well distributed between −900 and 0 bp in the upstream region of ovine *IFNT* (Supplemental Fig. S2). Results from our laboratory [23] revealed that the methylation status of ovine *IFNT* during active transcription was different from that during other periods when gene transcription was silenced. In fact, the upstream region of ovine *IFNT* in Day 14 sheep conceptuses, which had the highest levels of ovine *IFNT* mRNAs, was hypomethylated at CpG dinucleotides located in the upstream region (−1000 to −7 bp) of ovine *IFNT* (M88773). In contrast, ovine uterine endometrium and peripheral blood mononuclear cells, which do not express ovine *IFNT*, were hypermethylated at these CpG sites [23]. Five CpG sites found in the upstream region (−526 to −7 bp) of ovine *IFNT* are initially methylated as ovine *IFNT* transcription declines [23]. Therefore, it is likely that methylation to the 5′ flanking region of *IFNT* is one of the molecular mechanisms by which this gene is kept silent in tissues or cell types other than the peri-implantation conceptus.

In addition to DNA methylation, histone posttranslational modifications such as histone acetylation and methylation are involved in activation and/or repression of transcription. It has become apparent that gene transcription is regulated in a dynamic fashion rather than by on-and-off switches [24]. In this study, active transcription in bovine *IFNT* was found in CT-1 and BT-1 cells in which the degree of H3K18 acetylation was kept at high levels. Broad histone acetylation leads to partial decondensation of chromosomal domains, enabling various transcription factors to bind to DNA sequences. A DNA-bound activator in the promoter region then recruits positive modifiers such as CBP/p300, and DNA-bound RNA polymerase recruits histone methyltransferases at the ORF, resulting in increased H3K4 methylation to loosen chromatin structure and further promote transcription. In fact, H3K4 methylation on bovine *IFNT* was found in promoter and ORF regions of CT-1 cells, whereas it was found in the ORF region of TSA-treated MDBK cells but not in the TSA-nontreated MDBK cells (Fig. 3). These data suggest that, in addition to H3K18 acetylation, H3K4 methylation could also be associated with activation of bovine *IFNT* transcription in trophoblast cells.

In the "off" state of gene transcription, the DNA-bound repressor(s) at the repressor site recruits negative modifiers such as HDACs that remove acetyl groups from histones, resulting in condensation of chromosomal domains. Increased histone H3K9 methylation, especially H3K9 dimethylation,

also recruits repressing effector proteins such as HP1 and HDAC complexes that stabilize nucleosomes during transcription attenuation or repression [24]. Binding of HDACs in the upstream region of bovine *IFNT* suggests that histone deacetylation and possibly HDAC complex formation are involved in the silencing of *IFNT* expression in nontrophoblast cells. In TSA-treated MDBK cells, H3K18 acetylation and H3K4 trimethylation were increased, while H3K9 dimethylation was unchanged in upstream and ORF regions of bovine *IFNT*. Despite the fact that H3K18 acetylation was increased in MDBK cells that had been treated with TSA, bovine *IFNT* expression was not induced. Although histone acetylation loosens chromatin structure, this opening may not be tightly correlated with active transcription. Even in the euchromatin state, gene transcription is repressed where histone methyltransferases is recruited through interaction with CBX5 by tumor suppressor retinoblastoma protein RB1 [37]. However, endogenous bovine *IFNT* transcription was highest when TSA was applied and *Cdx2* was overexpressed in MDBK cells, resulting from maximal *Cdx2* mRNA expression (Fig. 5B). It was recently demonstrated that HDAC levels in the *DRA* promoter are reduced to 50% of control levels and remained stable following TSA treatment [38]. These authors indicated that reduced HDAC in the promoter region of the *DRA* gene following TSA administration results from intranuclear mobility of HDAC1 and HDAC2. These data suggest that sufficient removal of HDACs by TSA may have promoted abundant expression of transfected *Cdx2*, which facilitates formation of a positive modifier complex and the transcriptional coactivator CREBBP, which also exhibits HAT activity. In our previous study [19], overexpression of *Crebbp* increased the degree of ovine *IFNT* transcription, further supporting the notion that HAT activity is involved in *IFNT* transcription. These findings suggest that induction of endogenous *IFNT* transcription in bovine trophoblast cells results from partial decondensation of chromosomal domains by histone acetylation and sufficient CDX2 expression.

In conclusion, because 14 potential CDX2 binding sites were found in region 2 (−240 to −47 bp) of bovine *IFNT* and because TSA treatment and *Cdx2* overexpression were most effective in CDX2 binding in region 2 of bovine *IFNT* in nontrophoblast cells, we propose that active bovine *IFNT* transcription in trophoblast BT-1 and CT-1 cell lines results from the absence of HDACs and from sufficient CDX2 binding in region 2. Further experiments are required to elucidate whether this molecular mechanism is sufficient to explain in utero regulation of *IFNT* in bovine or ovine species.

ACKNOWLEDGMENTS

The authors thank Dr. Lutz Weber, Oak Ridge Institute for Science and Education, Oak Ridge, TN, for his critical reading of the manuscript. The authors also thank Drs. Alan Ealy (University of Florida, Gainesville, FL) and EunRan Suh (University of Pennsylvania School of Medicine, Philadelphia, PA) for generously providing bovine trophoblast CT-1 cells and the CDX2 expression plasmid, respectively.

REFERENCES

1. Roberts RM, Cross JC, Leaman DW. Interferons as hormones of pregnancy. Endocr Rev 1992; 13:432–452.
2. Imakawa K, Chang KT, Christenson RK. Pre-implantation conceptus and maternal uterine communications: molecular events leading to successful implantation. J Reprod Dev 2004; 50:155–169.
3. Vallet JL, Bazer FW, Fliss MF, Thatcher WW. Effect of ovine secretory proteins and purified ovine trophoblast protein-1 on interoestrous interval and plasma concentrations of prostaglandin F-2α and E and of 13, 14-dihydro-15-keto prostaglandin F-2α in cyclic ewes. J Reprod Fertil 1988; 84:493–504.
4. Spencer TE, Bazer FW. Ovine interferon tau suppresses transcription of the estrogen receptor and oxytocin receptor genes in the ovine endometrium. Endocrinology 1996; 137:1144–1147.
5. Godkin JD, Bazer FW, Moffatt J, Sessions JF, Roberts RM. Purification and properties of a major, low molecular weight protein released by the trophoblast of sheep blastocysts at day 13–21. J Reprod Fertil 1982; 65: 141–150.
6. Demmers KJ, Derecka K, Flint A. Trophoblast interferon and pregnancy. Reproduction 2001; 121:41–49.
7. Farin CE, Imakawa K, Roberts RM. In situ localization of mRNA for the interferon, ovine trophoblast protein-1, during early embryonic development of the sheep. Mol Endocrinol 1989; 3:1099–1107.
8. Guillomot M, Michel C, Gaye P, Charlier M, Trojan J, Martal J. Cellular localization of an embryonic interferon, ovine trophoblastin and its mRNA in sheep embryos during early pregnancy. Biol Cell 1990; 68:205–211.
9. Ashworth CJ, Bazer FW. Changes in ovine conceptus and endometrial function following asynchronous embryo transfer or administration of progesterone. Biol Reprod 1989; 40:425–433.
10. Gnatek GG, Smith LD, Duby RT, Godkin JD. Maternal recognition of pregnancy in the goat: effects of conceptus removal on interestrus intervals and characterization of conceptus protein production during early pregnancy. Biol Reprod 1989; 41:655–663.
11. Imakawa K, Hansen TR, Malathy PV, Anthony RV, Polites HG, Marotti KR, Roberts RM. Molecular cloning and characterization of complementary deoxyribonucleic acids corresponding to bovine trophoblast protein-1: a comparison with ovine trophoblast protein-1 and bovine interferon-αII. Mol Endocrinol 1989; 3:127–139.
12. Lifsey BD Jr, Baumback GA, Godkin JD. Isolation and immunocytochemical localization of bovine trophoblast protein-1. Biol Reprod 1989; 40:343–352.
13. Yamaguchi H, Ikeda Y, Moreno JI, Katsumura M, Miyazawa T, Takahashi E, Imakawa K, Sakai S, Christenson RK. Identification of a functional transcriptional factor AP-1 site in the sheep interferon tau gene that mediates a response to PMA in JEG3 cells. Biochem J 1999; 340: 767–773.
14. Yamaguchi H, Nagaoka K, Imakawa K, Sakai S, Christenson RK. Enhancer regions of ovine interferon-τ gene that confer PMA response or cell type specific transcription. Mol Cell Endocrinol 2001; 173:147–155.
15. Ezashi T, Ealy AD, Ostrowski MC, Roberts RM. Control of interferon-τ gene expression by Ets-2. Proc Natl Acad Sci U S A 1998; 95:7882–7887.
16. Ezashi T, Ghosh D, Roberts RM. Repression of Ets-2 induced transactivation of the interferon-τ promoter by Oct-4. Mol Cell Biol 2001; 21:7883–7891.
17. Sun Y, Duckworth ML. Identification of a placental-specific enhancer in the rat placental lactogen II gene that contains binding sites for members of the Ets and AP-1 (activator protein 1) families of transcription factors. Mol Endocrinol 1999; 13:385–399.
18. Matsuda F, Xu N, Kijima S, Tachi C, Christenson RK, Sakai S, Imakawa K. Analysis of transcriptional control elements in the 5′-upstream region of ovine interferon-τ gene using feeder-independent caprine trophoblast cell line, HTS-1. Placenta 2004; 25:166–175.
19. Xu N, Takahashi Y, Matsuda F, Sakai S, Christenson RK, Imakawa K. Coactivator CBP in the regulation of conceptus IFNτ gene transcription. Mol Reprod Dev 2003; 65:23–29.
20. Das P, Ezashi T, Gupta R, Roberts RM. Combinatorial roles of protein kinase A, Ets2, and 3′,5′-cyclic-adenosine monophosphate response element-binding protein-binding protein/p300 in the transcriptional control of interferon-tau expression in a trophoblast cell line. Mol Endocrinol 2008; 22:331–343.
21. Jaenisch R. DNA methylation and imprinting: why bother? Trends Genet 1997; 13:323–329.
22. Kass SU, Pruss D, Wolffe AP. How does DNA methylation repress transcription? Trends Genet 1997; 13:444–449.
23. Nojima H, Nagaoka K, Christenson RK, Shiota K, Imakawa K. Increase in DNA methylation downregulates conceptus interferon-tau gene expression. Mol Reprod Dev 2004; 67:396–405.
24. Berger SL. The complex language of chromatin regulation during transcription. Nature 2007; 447:407–412.
25. Kouzarides T, Berger SL. In: Allis CD, Jenuwein T, Reinberg D, Caparros ML (eds.), Epigenetics. New York: Cold Spring Harbor Press; 2006:191–209.
26. Soppe WJ, Jasencakova Z, Houben A, Kakutani T, Meister A, Huang MS, Jacobsen SE, Schubert I, Fransz PF. DNA methylation controls histone H3 lysine 9 methylation and heterochromatin assembly in Arabidopsis. EMBO J 2002; 21:6549–6559.
27. Bannister AJ, Zegerman P, Partridge JF, Miska EA, Thomas JO, Allshire

RC, Kouzarides T. Selective recognition of methylated lysine 9 on histone H3 by the HP1 chromo domain. Nature 2001; 410:120–124.
28. Lachner M, O'Carroll D, Rea S, Mechtler K, Jenuwein T. Methylation of histone H3 lysine 9 creates a binding site for HP1 proteins. Nature 2001; 410:116–120.
29. Briggs SD, Bryk M, Strahl BD, Cheung WL, Davie JK, Dent SY, Winston F, Allis CD. Histone H3 lysine 4 methylation is mediated by Set1 and required for cell growth and rDNA silencing in *Saccharomyces cerevisiae*. Genes Dev 2001; 15:3286–3295.
30. Degrelle SA, Campion E, Cabau C, Piumi F, Reinaud P, Richard C, Renard JP, Hue I. Molecular evidence for a critical period in mural trophoblast development in bovine trophoblasts. Dev Biol 2005; 288:448–460.
31. Imakawa K, Kim MS, Matsuda-Minehata F, Ishida S, Iizuka M, Suzuki M, Chang KT, Echternkamp SE, Christenson RK. Regulation of the ovine interferon-tau gene by a blastocyst-specific transcription factor, Cdx2. Mol Reprod Dev 2006; 73:559–567.
32. Shimada A, Nakano H, Takahashi T, Imai K, Hashizume K. Isolation and characterization of a bovine blastocyst-derived trophoblastic cell line, BT-1: development of a culture system in the absence of feeder cells. Placenta 2001; 22:652–662.
33. Talbot NC, Caperna TJ, Edwards JL, Garrett W, Wells KD, Ealy AD. Bovine trophoblast-derived trophectoderm and endoderm cell cultures: interferon tau and transferring expression as respective in vitro markers. Biol Reprod 2000; 62:235–247.
34. Livak KJ, Schmittgen TD. Analysis of relative gene expression data using real-time quantitative PCR and the $2^{-\Delta\Delta CT}$ method. Methods 2001; 25: 402–408.
35. Rings EH, Boudreau F, Taylor JK, Moffett J, Suh ER, Traber PG. Phosphorylation of the serine 60 residue within the Cdx2 activation domain mediates its transactivation capacity. Gastroenterology 2001; 121: 1437–1450.
36. Liu J, Puscheck EE, Wang F, Trostinskaia A, Barisic D, Maniere G, Wygle D, Zhong W, Rings EH, Rappolee DA. Serine-threonine kinases and transcription factors active in signal transduction are detected at high levels of phosphorylation during mitosis in preimplantation embryos and trophoblast stem cells. Reproduction 2004; 128:643–654.
37. Lachner M, Jenuwein T. The many faces of histone lysine methylation. Curr Opin Cell Biol 2002; 14:286–298.
38. Gialitakis M, Kretsovali A, Spilianakis C, Kravariti L, Mages J, Hoffmann R, Hatzopoulos AK, Papamatheakis J. Coordinated changes of histone modifications and HDAC mobilization regulate the induction of MHC class II genes by Trichostatin A. Nucleic Acids Res 2006; 34:765–772.